Few-Body Systems manuscript No.
(will be inserted by the editor)

Study of Generalized Parton Distributions at Jefferson Lab

Andrey Kim · for CLAS Collaboration

Received: date / Accepted: date

Abstract The quark-gluon dynamics manifests itself in a set of non-perturbative functions describing all possible spin-spin and spin-orbit correlations. The Generalized Parton Distributions (GPDs) carry information not only on the longitudinal momentum but also on the transverse position of partons, providing rich and direct information on the orbital motion of quarks. The hard exclusive production of photons and pions provide a variety of spin and azimuthal angle dependent observables, sensitive to the dynamics of quark-gluon interactions. The study of the GPDs is one of the main goals of Jefferson Lab 12 GeV upgrade. In this talk, we present an overview of the current status and some future measurements of hard exclusive processes and extraction of underlying GPDs at Jefferson Lab.

Keywords Nucleon structure · CLAS collaboration · Deeply Virtual Compton Scattering · Deeply Virtual Meson Production · Generalized parton distributions · Longitudinally polarized target

1 Introduction

In recent years, parton distribution functions have been generalized to contain information not only on the longitudinal but also on the transverse distributions of partons in a fast moving hadron. The Generalized Parton Distributions (GPDs) [1–3] add an important piece of information that is missing in one-dimensional parton densities, in particular, the distribution of partons in the plane transverse to the direction of motion. The most important aspect is that GPDs can provide detailed knowledge about the space-momentum distributions of quarks and gluons within the nucleon and about the contribution of

A. Kim
University of Connecticut
E-mail: kenjo@jlab.org

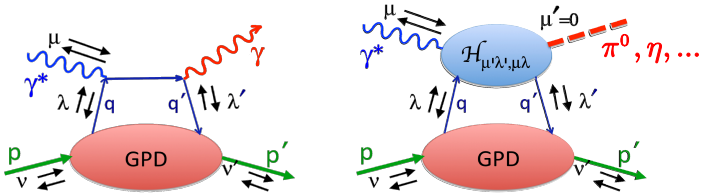

Fig. 1 Schematic DVCS (left) and DVMP (right) in the handbag mechanism framework. The helicities of initial (final) nucleon and quark are denoted as ν (ν') and λ (λ') respectively. The incident virtual photon and produced photon (meson) have μ and μ' helicities.

quark orbital angular momentum to the nucleon spin. GPDs contain the information needed to construct a multi-dimensional image of the internal structure of the nucleon.

Deeply virtual exclusive processes where the photon virtuality Q^2 is large, have emerged as a powerful probe to study the nucleon structure at the parton level. In the Bjorken scaling regime, the scattering amplitude of hard exclusive processes, such as Deeply Virtual Compton Scattering (DVCS) and Deeply Virtual Meson Production (DVMP), factorizes into a hard scattering part and soft part described by Generalized Parton Distributions. This opens the prospect of using exclusive meson electroproduction processes as a means to systematically explore the quark structure of the nucleon. Schematic illustrations for DVCS and DVMP in the handbag framework are shown on Fig. 1. While DVCS has most extensively been studied theoretically [4,5] and experimentally [6–9] to constrain the leading order GPDs, DVMP offers the advantage of filtering certain GPDs and also has evolved into an important process giving access to higher-twist mechanisms.

In general, there are four chiral-even GPDs (H, $\tilde{H}$, E, $\tilde{E}$) involved in the parton helicity-conserving processes and four chiral-odd GPDs that correspond to parton helicity-flip processes (H_T, $\tilde{H}_T$, E_T, $\tilde{E}_T$). They depend on three kinematic variables: x, ξ and t, where x is the average parton longitudinal momentum fraction and ξ (skewness) is half of the longitudinal momentum fraction transferred to the struck parton. The skewness can be expressed in terms of the Bjorken variable x_B as $\xi \simeq x_B/(2-x_B)$, in which $x_B = Q^2/(2pq)$, q is the four-momentum of the virtual photon and $Q^2 = -q^2$. The momentum transfer to the nucleon is $t = (p-p')^2$, where p and p' are the initial and final four momenta of the nucleon. At leading twist of the GPD framework, DVCS amplitudes couple only to transverse photons and is sensitive to chiral-even GPDs H, $\tilde{H}$ and E, while the neutral pseudoscalar DVMP amplitudes couple only to longitudinally polarized photons and these channels are sensitive only to the chiral even GPDs $\tilde{H}$, $\tilde{E}$ in the nucleon [10,11]. The last two GPDs contain information about the spatial distribution of the quark spin. The early theoretical efforts to explain the pseudoscalar DVMP focused on these $\tilde{H}$ and $\tilde{E}$ GPDs at leading twist. However, Hall-B at Jefferson Lab measured surprisingly large π^0 beam spin asymmetry (BSA) values that strongly suggest

substantial contributions from transversely polarized photons [12], otherwise the BSA should be zero or very small. These contributions can be calculated within a handbag approach as the convolutions of leading-twist chiral-odd GPDs with a twist-3 meson distribution amplitude [13–15]. The recent publication of CLAS collaboration on measurements of exclusive π^0 electroproduction structure functions [16] showed strong sensitivity to transversity GPDs.

2 Deeply Virtual Compton Scattering

The JLab Hall A collaboration presented first measurements of the $ep \to ep\gamma$ cross sections in the valence quark region [17]. The experiment E00-110 ran in Hall A [18] at JLab with a 5.75 GeV longitudinally polarized electron beam and a 15-cm-liquid H_2 target. As it is impossible to separate Bethe-Heitler (BH) and DVCS processes experimentally one measures both processes, as well as their interference, and then removes the contribution from the pure BH term as it is exactly calculable in terms of the nucleon form factors [3, 19]. The cross sections for DVCS on proton were measured for three kinematic points at Q^2=1.5, 1.9 and 2.3 GeV^2. The DVCS helicity-independent and helicity-dependent cross sections provide access to the real and imaginary part of BH-DVCS interference term respectively. The azimuthal dependence of the helicity-dependent cross section allows the separation of twist-2 and twist-3 contributions in the DVCS-BH interference terms. Fig. 2(left) shows the Q^2 dependence of the imaginary angular harmonics over the full t domain. The

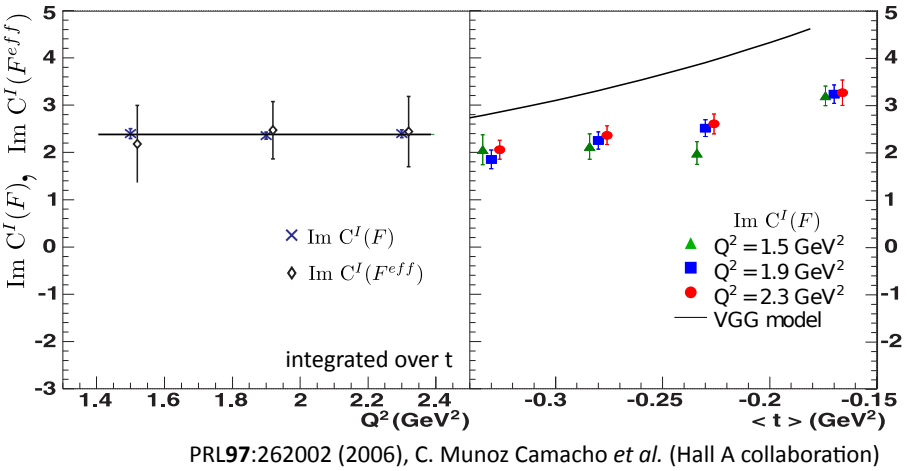

Fig. 2 Left: Q^2 dependence of imaginary parts of (twist-2) $C^I(F)$ and (twist-3) $C^I(F^{eff})$ angular harmonics, averaged over t. The horizontal line is the fitted average of Im$[C^I(F)]$). Right: Extracted imaginary parts of the twist-2 angular harmonics as a function of t. The theoretical predictions are from the Ref. [20,19,21].

right plot displays the twist-2 angular harmonics as a functions of t, together

with the predictions from a model of Vanderhaeghen, Guichon and Guidal (VGG) [20,19,21]. The absence of Q^2 dependence provides crucial support for the dominance of the twist-2 in DVCS amplitude at modest Q^2.

The JLab CLAS collaboration measured beam spin asymmetry (BSA) [22] (see Fig. 3) and cross sections [23] in the reaction $\mathbf{e}p \to ep\gamma$ using a longitudinally polarized electron beam with 5.77 GeV energy, 2.5 cm-long liquid-hydrogen target and CLAS spectrometer [24]. Neglecting a twist-3 DVCS term, the BSA arises from the interference from BH and DVCS processes that is sensitive to the specific combination of the proton GPDs H, $\tilde{H}$ and E. The GPD H provides the dominant contribution to the beam spin asymmetry, thus, neglecting the small contribution from other GPDs, BSA can be expressed as a function of only H.

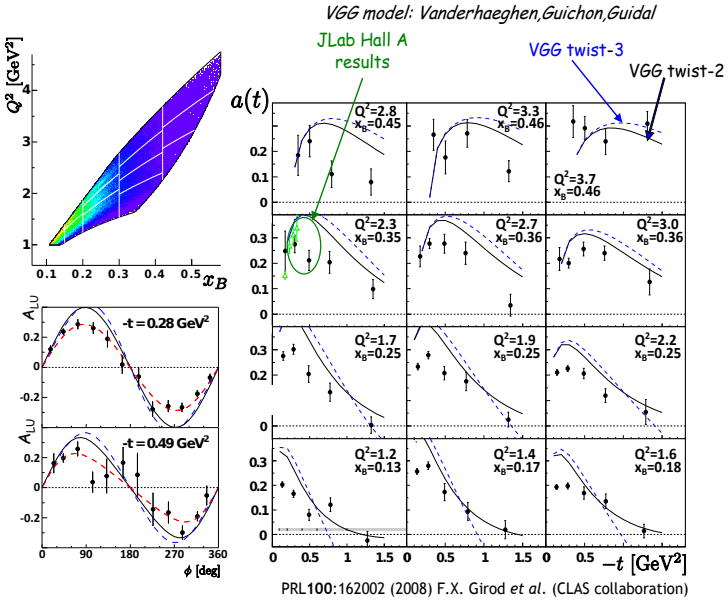

Fig. 3 Left top panel shows the kinematic coverage and binning in Q^2, x_B space. Left bottom panel shows the beam spin asymmetries as a function of ϕ for two of the 62 (Q^2, x_B, t) bins corresponding to the $\langle x_B \rangle = 0.25$, $\langle Q^2 \rangle = 1.95$ GeV^2 and two values of $\langle t \rangle$. Right: beam spin asymmetries at 90° as a function of $-t$. Each individual plot corresponds to a bin in Q^2, x_B. The red-dashed curves correspond to the fit. The black (blue) curves correspond to the GPD calculation at twist-2 (twist-3) levels, with H contribution only.

The first measurements of longitudinal target spin asymmetries (TSA) were published by the CLAS collaboration [25] (see Fig. 4) using 5.7 GeV electron beam and longitudinally polarized NH_3 target. A significant azimuthal dependence of BH-DVCS interference term yields directly to the dominant combination of GPDs H and $\tilde{H}$, with other GPDs being kinematically suppressed.

The wide kinematic coverage of CLAS is particularly important as it allows the global analysis of measured observables and a model-independent extrac-

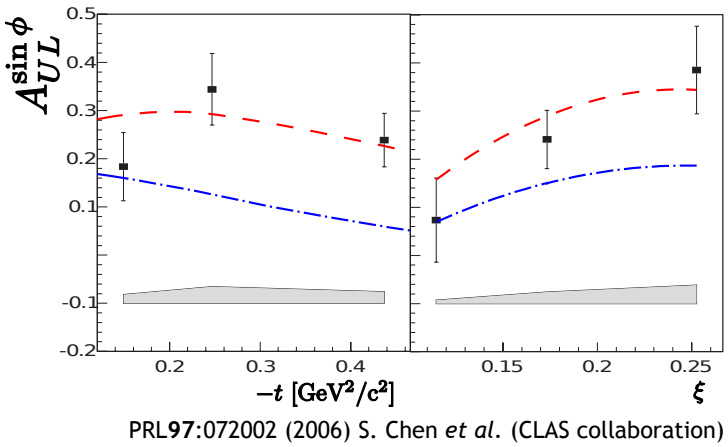

Fig. 4 The $-t$ (left) and ξ (right) dependence of the $\sin\phi$ moment of target spin asymmetry for DVCS. The dashed curves represent VGG model predictions using ξ-dependent GPD parametrization. The dotted curves show the asymmetries when $\tilde{H}$=0.

tion of DVCS amplitudes. For example, BSA is especially sensitive to the GPD H. Combined with TSA that is sensitive to H and $\tilde{H}$, it allows to constrain the contribution from $\tilde{H}$ alone.

3 Deeply Virtual π^0 Production

Although DVCS is the cleanest process to access GPDs, the variety of DVMP channels allows to perform quark flavor separation of GPDs. In addition, pseudoscalar meson electroproduction, particularly π^0 production in the reaction $ep \to e'p'\pi^0$, was identified as especially sensitive to the parton helicity-flip subprocesses. While the interpretation of π^+ production is complicated by the dominance of the longitudinal π^+-pole term, the π^0 production, where that contribution is absent, may become a unique source of information on transversity GPDs [26,14].

Beam spin asymmetries for exclusive π^0 electroproduction were measured by the CLAS collaboration in a wide kinematic range [27]. The measured asymmetries are of the order of 0.04 to 0.11, and, in particular, show no decrease as a function of Q^2. This is a clear sign of significant contribution from LT' interference, that can not be calculated within the formalism where only longitudinal amplitude, dominant in the Bjorken regime, is considered. These nonzero asymmetries imply that both transverse and longitudinal amplitudes participate in the process.

During the past few years, two parallel approaches have been developed utilizing chiral odd GPDs in the calculation of pseudoscalar electroproduction: the Goloskokov-Kroll (GK) model [28,26,14] and Goldstein-Liuti (GL) model [29]. Although different in details they both lead to sizable transverse photon amplitudes, as evidenced in the CLAS data and recent measurements by Hall

A collaboration [30]. Inclusion of the chirally-odd components of the hard exclusive amplitude gives results in fair agreement with the measured cross sections [31] (see Fig. 5). A combination of $\widetilde{H}_T$ and E_T plays a particularly prominent role. The cross section behaviour in the low $-t$ region is determined by interplay between these two GPDs. The comparison between data and model predictions shows the sensitivity of the measured π^0 structure functions to chiral-odd GPDs.

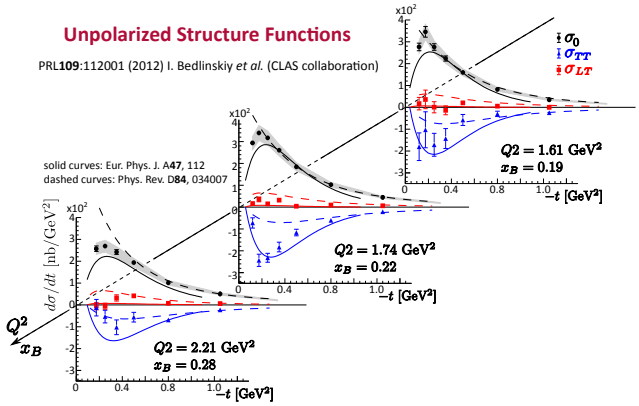

Fig. 5 The extracted structure functions for exclusive π^0 electroproduction as a function of t for the bins with best kinematic coverage. The curves are theoretical predictions and explained on the graph. The shaded bands represent experimental systematic uncertainties.

In parallel, cross sections and structure functions for $ep \to ep\eta$ were also obtained. The comparison of the π^0 and preliminary η structure functions is shown on Fig. 6. σ_U drops by a factor of 2.5 for η-mesons in comparison with π^0 and σ_{TT} drops by a factor of 10. The GK GPD model (curves) follows the experimental data. The inclusion of η data into consideration strengthens the statement about the transversity GPD dominance in the pseudoscalar electroproduction process. Combined π^0 and η data open the way for the flavor decomposition of the underlying transversity GPDs.

The analysis of experimental data on exlusive π^0 electroproduction is underway to extract longitudinal target spin asymmetries as well as double spin asymmetries. The experiment ran in 2009 in Hall B, JLab using longitudinally polarized electron beam and longitudinally polarized solid NH_3 target. The unpolarized and polarized structure functions can be expressed as a combination of the partonic subprocess amplitudes and GPDs convolutions. Therefore measurements of beam, target and double spin asymmetries and extraction of azimuthal moments provide several observables, combined analysis of which may allow separation of contributions from different underlying GPDs.

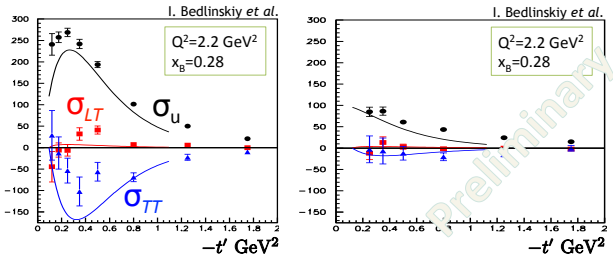

Fig. 6 Structure function $\sigma_T + \epsilon\sigma_L$ (black), σ_{TT} (blue) and σ_{LT} (red) as a function of $-t$ for π^0 (left) and η (right) exclusive electroproduction for kinematic point (Q^2 =2.2 GeV^2, x_B =0.28). Data points: CLAS, preliminary. Curves: theoretical predictions produced with GK handbag model.

4 Conclusion

The dedicated experiments to measure DVCS and DVMP at Jefferson Lab with 6 GeV electron beam provide a large set of experimental data over a wide kinematic range. Combined together they allow access to chiral even as well as chiral odd GPDs. The initial interpretations of deep exclusive processes in terms of Generalized Parton Distributions models are already showing remarkable results.

The successful description of unpolarized cross sections for pseudoscalar meson production by CLAS provides a unique opportunity to access chiral odd GPDs. The precise calculations of polarized spin observables, however, are not feasible at present. Theoretical calculations of π^0 electroproduction based on the GPDs inspired models include many uncertainties such as parametrization of the chiral odd GPDs, treatment of the higher twist contributions and the reaction mechanisms (*e.g.*, corrections to the partonic mechanism from hadronic–size configurations in high–Q^2 production). The extractions of structure functions for various DVMP channels would increase the number of experimental observables used for model-independent constraints and further clarify the discrepancies between data and model calculations.

The work presented here leads directly to the program of the Jefferson Lab 12 GeV upgrade. The increased energy and luminosity will allow higher accuracy measurements over significantly wider kinematic range providing us with the opportunity to extend our analysis at higher Q^2 and test the mechanism of exclusive photon and meson electroproduction.

Acknowledgements We acknowledge the outstanding efforts of the staff of the Accelerator and Physics Divisions at JLab. This work was supported in part by the U.S. Department of Energy and National Science Foundation, the French Centre National de la Recherche Scientifique and Commissariat à l'Energie Atomique, the Italian Istituto Nazionale di Fisica Nucleare, the National Research Foundation of Korea and the U.K. Engineering and Physical Science Research Council. Jefferson Science Associates (JSA) operates the Thomas Jefferson National Accelerator Facility for the United States Department of Energy under contract DE-AC05-06OR23177.

References

1. X.D. Ji, Phys. Rev. Lett. **78**, 610 (1997)
2. A.V. Radyushkin, Phys. Lett. **B380**, 417 (1996)
3. A.V. Belitsky, D. Mueller, A. Kirchner, Nucl. Phys. **B629**, 323 (2002)
4. A. Radyushkin, Phys. Rev. D **56**, 5524 (1997)
5. D. Mueller, et al., Fortsch. Phys. **42**, 101 (1994)
6. S. Stepanyan, et al., Phys. Rev. Lett. **87**, 182001 (2001)
7. C. Camacho, et al., Phys. Rev. Lett. **97**, 262002 (2006)
8. F. Girod, et al., Phys. Rev. Lett. **100**, 162002 (2008)
9. G. Gavalian, et al., Phys. Rev. C **80**, 035206 (2009)
10. M.I. Eides, L.L. Frankfurt, M.I. Strikman, Phys.Rev. **D59**, 114025 (1999)
11. L. Mankiewicz, et al., Eur. Phys. J. C **10**, 307 (1999)
12. R. De Masi, et al., Phys. Rev. C **77**, 042201 (2008)
13. S. Ahmad, G.R. Goldstein, S. Liuti, Phys. Rev. **D79**, 054014 (2009)
14. S. Goloskokov, P. Kroll, Eur.Phys.J. **A47**, 112 (2011)
15. G.R. Goldstein, J.O.G. Hernandez, S. Liuti, Phys. Rev. D **84**, 034007 (2011)
16. I. Bedlinskiy, et al., Phys. Rev. Lett. **109**, 112001 (2012)
17. C. Munoz Camacho, et al., Phys. Rev. Lett. **97**, 262002 (2006)
18. J. Alcorn, B. Anderson, K. Aniol, J. Annand, L. Auerbach, et al., Nucl.Instrum.Meth. **A522**, 294 (2004)
19. K. Goeke, M.V. Polyakov, M. Vanderhaeghen, Prog. Part. Nucl. Phys. **47**, 401 (2001)
20. M. Vanderhaeghen, P.A.M. Guichon, M. Guidal, Phys. Rev. **D60**, 094017 (1999)
21. M. Guidal, M.V. Polyakov, A.V. Radyushkin, M. Vanderhaeghen, Phys. Rev. **D72**, 054013 (2005)
22. F.X. Girod, et al., Phys. Rev. Lett. **100**, 162002 (2008)
23. H.S. Jo, et al., Phys. Rev. Lett. **115**, 212003 (2015)
24. B. Mecking, et al., Nucl.Instrum.Meth. **A503**, 513 (2003)
25. S. Chen, H. Avakian, V. Burkert, et al., Phys. Rev. Lett. **97**, 072002 (2006)
26. S.V. Goloskokov, P. Kroll, Eur. Phys. J. **C65**, 137 (2010)
27. R. De Masi, et al., Phys.Rev. **C77**, 042201 (2008)
28. S.V. Goloskokov, P. Kroll, Eur. Phys. J. **C53**, 367 (2008)
29. G. Goldstein, J.O.G. Hernandez, S. Liuti, to be published (2013)
30. M. Defurne, et al., Phys. Rev. Lett. **117**, 262001 (2016)
31. I. Bedlinskiy, et al., Phys.Rev.Lett. **109**, 112001 (2012)